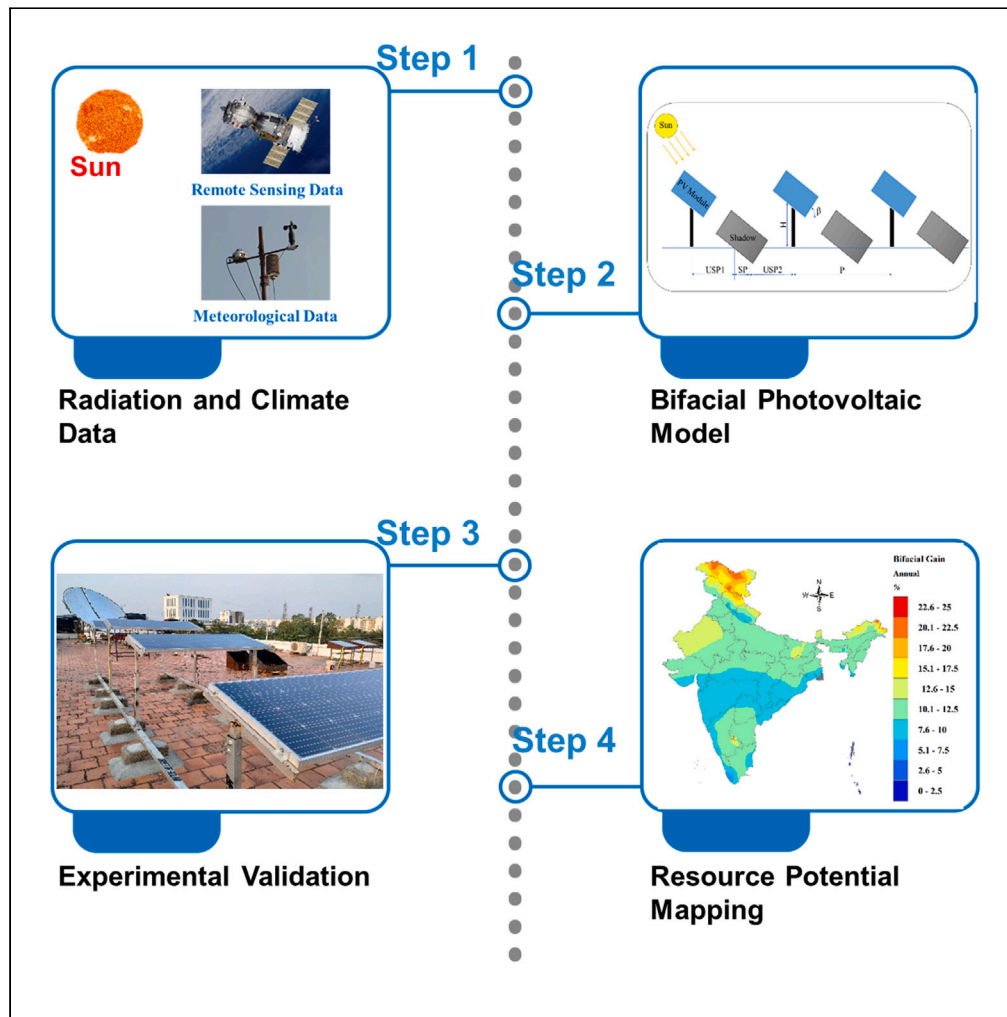


Article

Resource potential mapping of bifacial photovoltaic systems in India



Joji Johnson, S. Manikandan

jojij@srmist.edu.in (J.J.)
manikans@srmist.edu.in (S.M.)

Highlights

Developed maps to predict the performance of bifacial PV in India

Average annual bifacial gain for India is found to be 2.5%–22%

The highest annual average bifacial gain is in the north zone of India



Article

Resource potential mapping of bifacial photovoltaic systems in India

Joji Johnson^{1,*} and S. Manikandan^{1,2,*}

SUMMARY

Bifacial photovoltaic is one of the technologies that can spearhead Indian ambitions to achieve the 7th United Nations Sustainable Development Goals and Nationally Determined Contributions of COP 26. But, like all emerging technology, the lack of awareness and unavailability of extensive data, like technology potential maps that could aid people in identifying the advantages of newer technologies, has led to sluggish growth in the Indian market. To expedite the growth of bifacial PV in the Indian market, optimized resource potential maps of bifacial PV were developed from an experimentally validated view factor-based bifacial PV model. The annual average bifacial gain was found to vary between 2.5% and 22% at various locations in India. The effect of ground albedo and height of installation was also studied. Furthermore, the annual and seasonal power out of bifacial PV was higher than monofacial PV at any location in India.

INTRODUCTION

The 7th United Nations Sustainable Development Goal (UN SDG) is to ensure access to sustainable, affordable, and reliable modern energy for everyone on the planet by 2030 and net-zero emissions by 2050.¹ India has pledged to attain the goal by substantially increasing the share of renewable energy in the global energy mix and by doubling the global rate of improvement in energy efficiency by 2030. NITI Aayog reports on the progress of UN SDG goals and states that expanding infrastructure and upgrading technology is critical to attaining the 7th goal.² In addition, at the Climate Change Conference (COP 26), India pledged to reduce the emissions intensity of its gross domestic product by 45% by 2030 and to achieve about 50% cumulative electric power installed capacity from non-fossil fuel-based energy resources by 2030.³ The Indian government has instilled favorable policies and considerable investments in the renewable energy sector in the past decade, with solar power installed capacity of 61.97 GW as of 30th November 2022.⁴ Still, it requires heavy investment to attain its ambitious UN SDG and Nationally Determined Contributions of COP 26.

Photovoltaic (PV) power plants have a life of 25 years. However, due to degradation, there is a drop in the efficiency by between 0.16%/year and 1.72%/year of PV power plants in India, over a period of ten years, leading to a reduction in power output in the later stages of power plant life cycle.⁵ All India Survey of Photovoltaic Module Reliability for 1094 crystalline silicon PV modules at various locations throughout India gives the average or mean of overall degradation rate in maximum power output is 1.93%/year, and average linear degradation rate of maximum power output is 1.47%/year. The 1.47%/year average linear degradation rate of crystalline silicon PV modules is much higher than the international benchmark of 0.6%–0.8%/year. These alarmingly high degradation rates in India were due to large volume of installation, aggressive pricing and timelines, and improper handling/installation; all leading to the installation of poor-quality modules.⁶ Also, in the past decade, the cost of PV panels has decreased considerably while the cost of land has increased. Intensive research on PV has led to the development of bifacial modules that yields higher energy per unit area.⁷ Replacing the low-performing modules of existing monofacial power plants by good-quality bifacial PV can help attain lower levelized cost of electricity due to higher power production without compromising on PV panel quality and using bifacial PV modules in newer installations can aid India in achieving its UN SDG goals by utilizing the lesser amount of precious land which could otherwise be repurposed.⁸

Bifacial photovoltaic is a promising technology that can generate more power than conventional monofacial photovoltaic technology by absorbing solar radiation on both the front and rear sides of the photovoltaic panel.⁹ The worldwide installations of bifacial PV are projected to be 20 GW in 2020. Bifacial gain is the ratio of the additional power generated by the bifacial PV to the power generated by the monofacial PV. The annual energy yield of fixed tilt bifacial PV is up to 30%, and a single axis tracked is up to 40% greater than monofacial PV systems.¹⁰ The bifacial gain is higher under diffused illumination. However, the overall power output under diffused illumination is lower than on a sunny day.¹¹ The bifacial PV under low irradiance conditions on cloudy days has higher bifacial gain of 16.54% compared to 13.08% on sunny days.¹² This will aid in uniform power output and better grid stability under varying climatic conditions for a bifacial PV than a monofacial PV system. Bifacial PV is one of the most cost-effective PV solutions and is becoming one of the best technologies for power generation. The International

¹Department of Mechanical Engineering, Faculty of Engineering and Technology, SRM Institute of Science and Technology, Kattankulathur, Tamil Nadu 603203, India

²Lead contact

*Correspondence: jojij@srmist.edu.in (J.J.), manikans@srmist.edu.in (S.M.)

<https://doi.org/10.1016/j.isci.2023.108017>



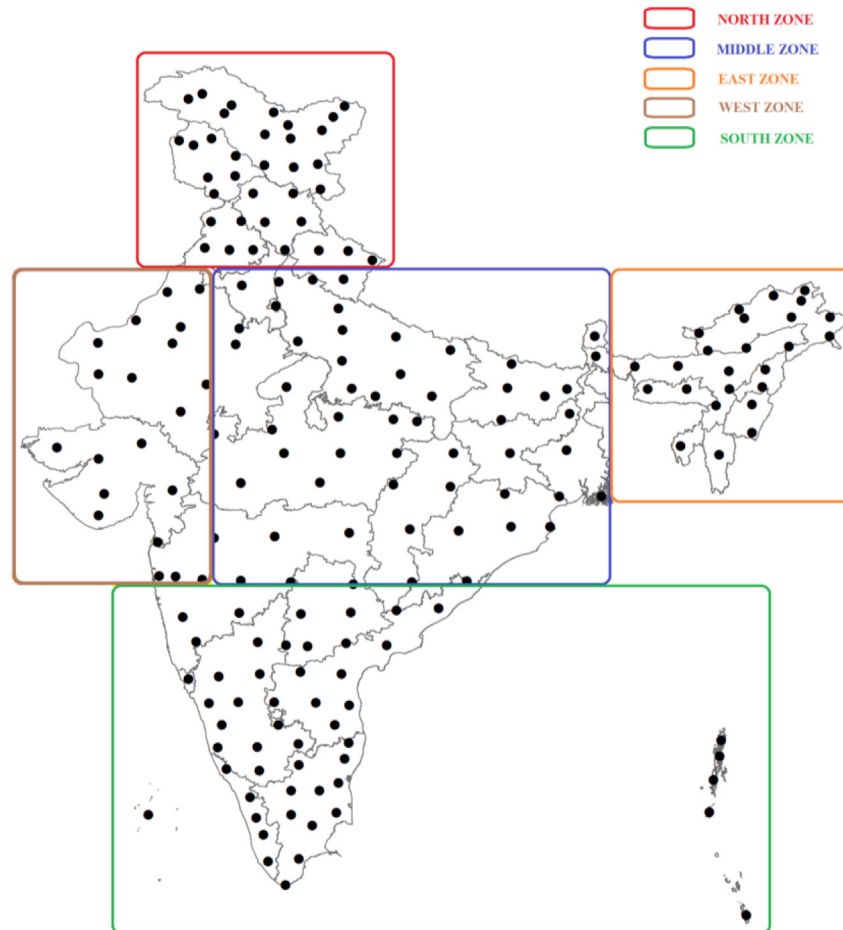


Figure 1. Geographical distribution of 188 locations

Technology Roadmap for Photovoltaic predicts the dominance of bifacial PV cells, with its market share increasing from 50% in 2021 to 85% within the next ten years.¹³

Even though bifacial PV is an old technology,¹⁴ the development and implementation of the technology attained momentum only a few years before. New developments in the open metallization grid, texturized wafers, and passivating anti-reflective at industrial production scales^{15–17} have led to the development of highly efficient bifacial PV cells.¹⁸ Like all newly inducted technologies, the acceptance of bifacial PV technology in the photovoltaic market is currently facing a critical challenge due to the bifacial PV production uncertainties and inadequate performance data of modules.¹⁹ The faster pace of research, more installations, and good bifacial PV performance, even at low albedo conditions, have led to speedier induction bifacial technology in Nordic countries at altitudes above 65°^{11,20} and USA.²¹ However, in India, the limitations in accurate prediction for forecasting the output of bifacial PV and the lack of public awareness are creating a struggle for the industry.¹⁹ The price of Bifacial PV is comparable to high-performance monofacial PV, at around 26.4 USD cents/Wp for bifacial monocrystalline p-type PERC solar modules.^{22,23} The bifacial PV also has slightly higher equipment and installation cost, but it is not excessive.²⁴ Also, unlike matured technology of monofacial PV, which has guidelines on physics-based standard calculators based on location to suggest tilt and the orientation of installation to optimize the power output, the bifacial technology is yet to generate sufficient onsite data to develop optimized calculators.^{25,26} To compensate for the unavailability of data, a mathematical model was developed to predict location-based bifacial performance.

A few pieces of literature are available predicting the worldwide techno-economics of bifacial PV.^{23,27} However, a detailed location-based technical estimate to optimize the performance of bifacial PV is not available for a large country like India. The performance of bifacial PV at any location depends on multiple parameters like slope, height, pitch, and albedo and also varies with climatic conditions and seasons.^{28,29} A map for India predicting the feasibility of the bifacial PV at any location is currently unavailable. This map can help boost the rate of adaptation of bifacial PV technology in the Indian market, similar to solar power potential maps developed for monofacial PV.^{30,31} So, resource maps need to be developed to predict the potential of bifacial PV in India to attract and aid prospective customers in understanding the benefits of bifacial PV technology.

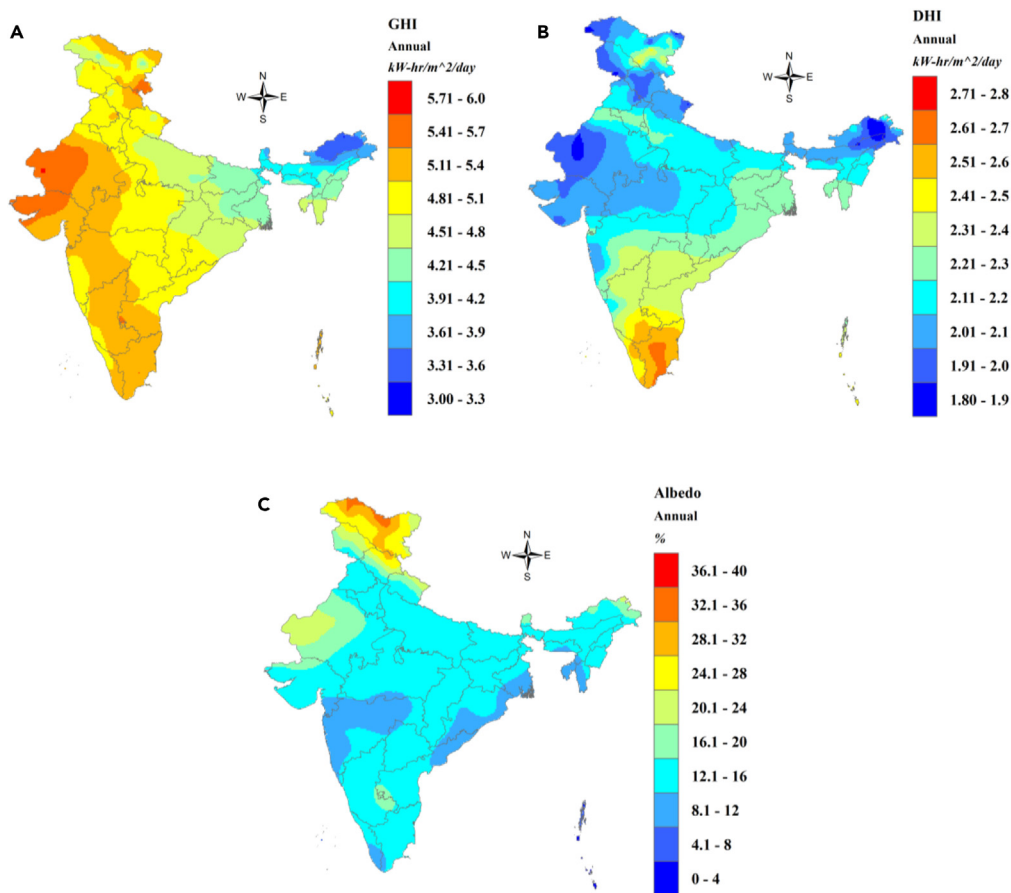


Figure 2. Solar radiation and albedo conditions for India

- (A) Global horizontal irradiance (GHI).
- (B) Diffuse horizontal irradiance (DHI).
- (C) Ground albedo.

In this article, an experimentally validated new view factor model was developed to predict the power output and bifacial gain of bifacial PV. Bifacial PV data were generated for 188 locations spread across India and input into ArcMap software to develop bifacial PV maps.³²

RESULTS

India is a huge country with widespread land mass, leading to varying solar energy potential. For the current analysis, the country is divided into five zones, as shown in Figure 1, to better analyze and elucidate the bifacial PV resource maps.

Radiation data maps

The map for daily average annual global horizontal irradiance and diffuse horizontal irradiance incidents in India in $\text{kWh/m}^2/\text{day}$ during the year 2020 is plotted from annual data in Power Data Access Viewer³³ as in Figures 2A and 2B, respectively. These maps show the daily average solar energy resources potential in India. It can be observed that the west and south zones have the highest and the east zone has the lowest

Table 1. Optimal model parametric specification

Specification	Value
Tilt angle/Slope (β)	Latitude angle
Height of installation/Elevation (h_0)	1.5 m
Pitch (PO)	2 m
Surface azimuth (γ)	0° (South facing)
Ground coverage ratio (GCR)	0.4

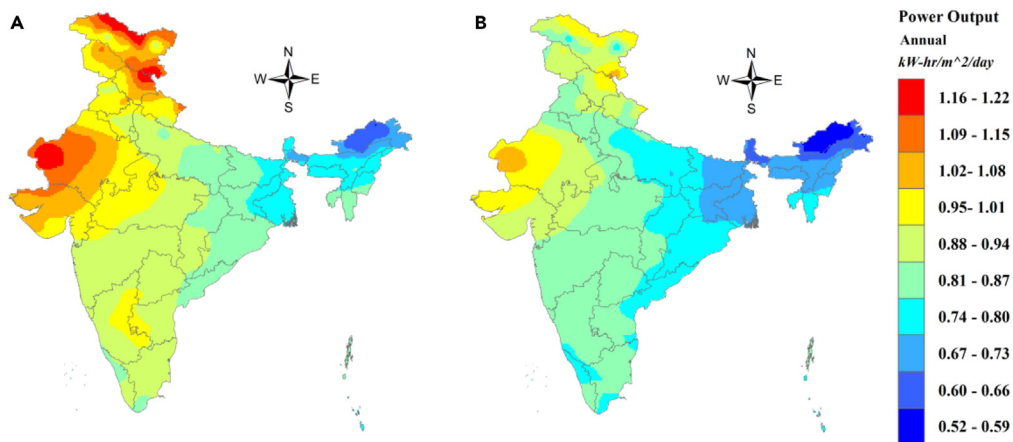


Figure 3. Daily average annual power output maps of India

(A) Daily average annual bifacial power output.

(B) Daily average annual monofacial power output.

solar potential. The ground albedo at any location varies seasonally and the characteristics of ground at various seasons i.e., grass cover, mud, snow, etc. Monthly average ground albedo at all locations is obtained from Power Data Access Viewer.³³ The average annual ground albedo is plotted in Figure 2C. This plot is similar to the map developed for ground albedo in NASA Visible Earth catalog.^{34,35} It can be observed that the ground albedo is maximum in the Himalayas due to snow cover and the average annual albedo is between 12.1% and 16% at most locations in India.

Optimal parameters of installation

Numerous simulations of various parameters were done to identify the optimal parameters of installation for bifacial PV as given in Table 1. The ground coverage ratio (GCR) is taken as the ratio of the PV modules area to the total ground area. Taking different sizes of module into

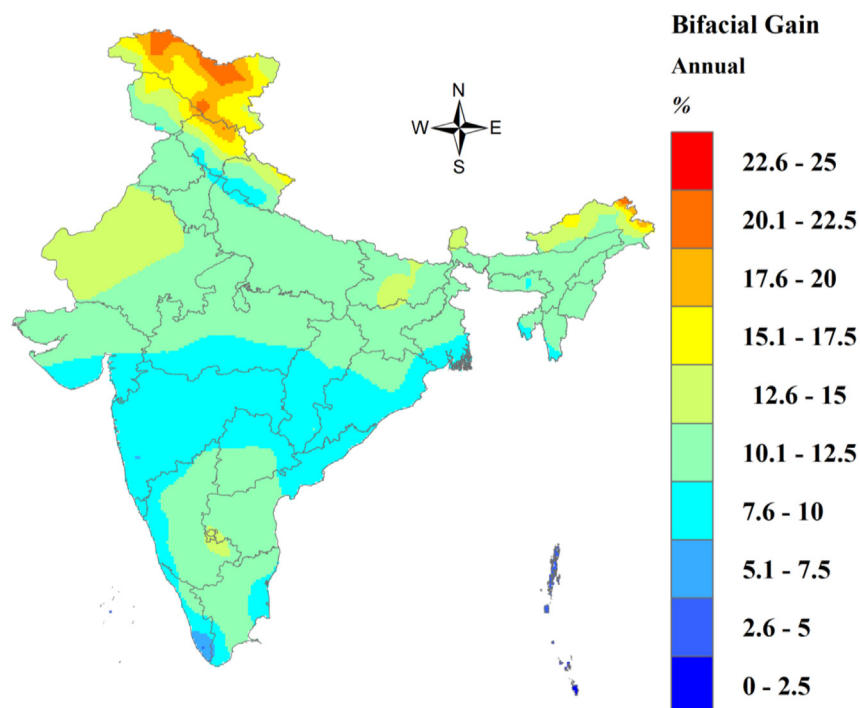


Figure 4. Average annual bifacial gain

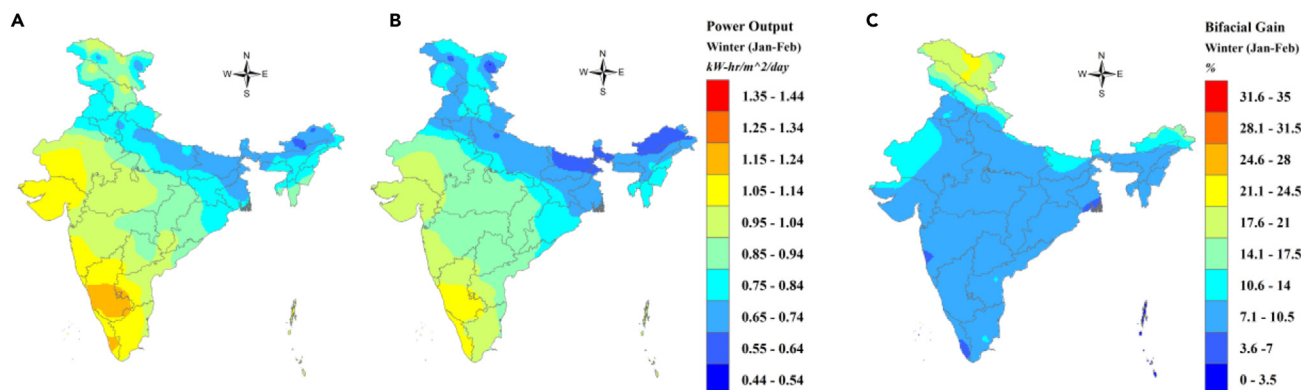


Figure 5. Power output and bifacial gain maps for the winter season in India (Jan–Feb)

- (A) Bifacial power output.
- (B) Monofacial power output.
- (C) Bifacial gain.

account, GCR is optimized as 0.4, taking cost of land and self-shading into account. Based on the panel size, the pitch can be optimized. The ground albedo is taken from the Power Data Access Viewer for that location.³³ The same parameters were also considered in the simulation of monofacial PV.

Daily average power output and bifacial gain

The annual radiation data are input into the model to develop the daily average monofacial and bifacial power output. Figure 3A represents the map of the daily average annual bifacial power output. The daily average bifacial power output potential annually varies between 0.6 and 1.2 kWh/m²/day. A similar distribution pattern is observed in the annual daily average power output of monofacial PV represented in Figure 3B with values between 0.5 and 1 kWh/m²/day. The annual daily average bifacial power output is higher for a bifacial PV compared to the monofacial PV at the same location. The lowest bifacial power generation potential is in the east zone of India, while the highest is in the west zone and parts of the north zone of India.

Figure 4 shows India's average annual bifacial gain for bifacial PV panels compared to monofacial PV panels. The bifacial gain varies between 2.4% and 22.3% at the optimal installation parameters conditions. The highest annual average bifacial gain is in the north zone of India, while the lowest gain is in the Andaman and Nicobar Islands in the south zone of India. The higher values of bifacial gain in the northern region are due to higher albedo values due to snow-covered ground in the Himalayas and vice versa for lower values of bifacial gain in the islands of south zone of India due to the lower albedo by green vegetation and water surrounding the islands. The PV panels are assumed to be regularly cleaned and maintained (snow/dust deposition neglected) in the development of these maps.

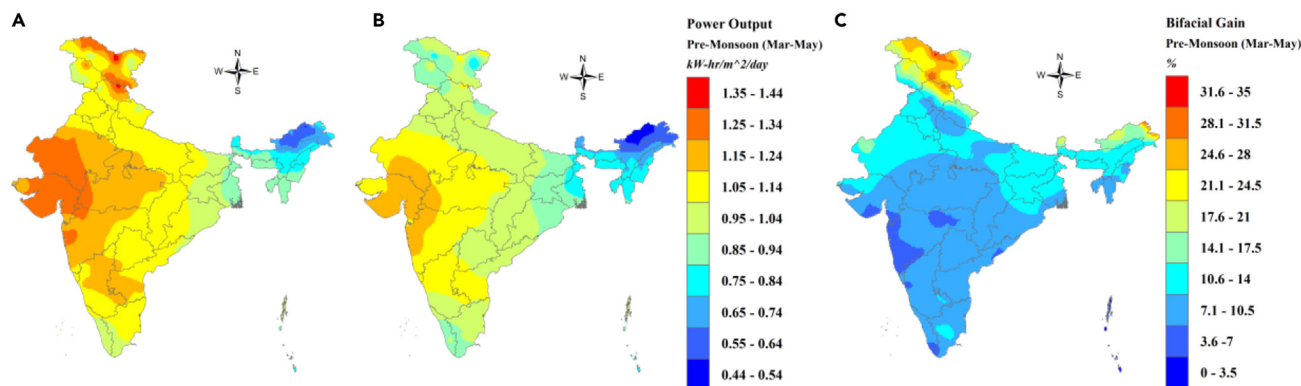


Figure 6. Power output and bifacial gain maps for the pre-monsoon season in India (Mar–May)

- (A) Bifacial power output.
- (B) Monofacial power output.
- (C) Bifacial gain.

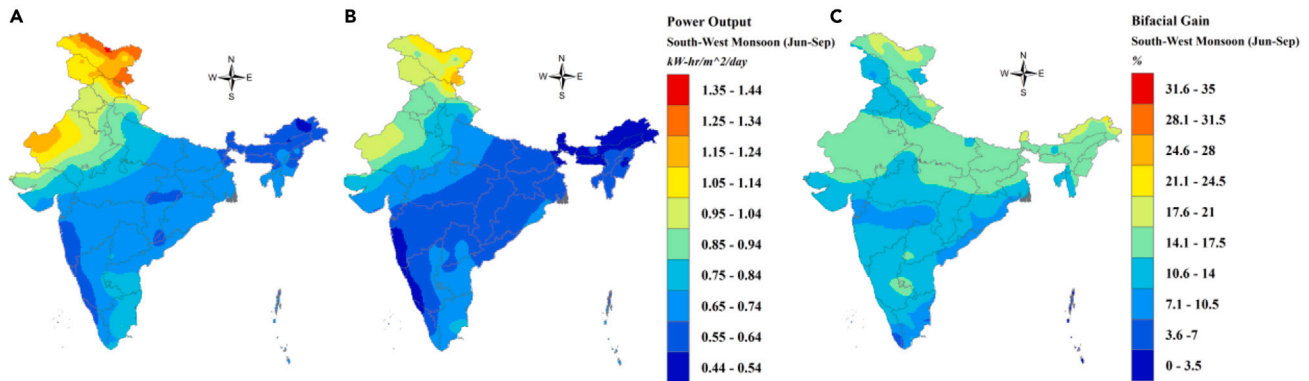


Figure 7. Power output and bifacial gain maps for the south-west monsoon season in India (Jun-Sep)

- (A) Bifacial power output.
- (B) Monofacial power output.
- (C) Bifacial gain.

Seasonal performance of bifacial PV

India has four major seasons:³⁶ winter season (January–February), pre-monsoon season (March–May), south-west monsoon season (June–September), and post-monsoon season (October–December). Seasonal maps are developed to predict the performance of monofacial and bifacial PV during various climatic conditions or seasons.

Figures 5, 6, 7, and 8 show the seasonal variation in bifacial power output, monofacial power output, and bifacial gain. The highest bifacial power output of $1.42 \text{ kWh/m}^2/\text{day}$ and bifacial gain of 32.5% was obtained during the pre-monsoon season, while the least bifacial power generation of $0.52 \text{ kWh/m}^2/\text{day}$ occurs in the south-west monsoon season. The bifacial power generation drops by an average of 25% in the south-west monsoon months of June to September compared to pre-monsoon months of March to May.

The range of bifacial gain at various zones in India is given in Table 2. The range is color coded based on the average value of the bifacial gain in that zone. The highest range of values for bifacial gain in all zones except the north zone is during the south-west monsoon season. South-west monsoon is usually rainy season with lots of cloud cover on the horizon. This shows that the bifacial modules have better bifacial gain in cloudy conditions. This is achieved by the higher fraction of diffuse light falling on the rear side of the bifacial PV during this season.

Effect of ground albedo

The ground albedo at different locations varies with the type of surface on which the panels are installed. Table 3 represents the albedo of different types of surfaces.³⁷

At any location, the surface of installation of PV panels may vary (roof top, sand, grass, etc.) and since the bifacial gain varies with ground albedo, maps for bifacial gain for varying albedo were developed for India. This was done by keeping other parameters in the optimal model fixed and varying the ground albedo values from 5% to 40%. From the simulations Figures 9A–9H, it is found that the bifacial gain proportionally increases with an increase in ground albedo at any location.

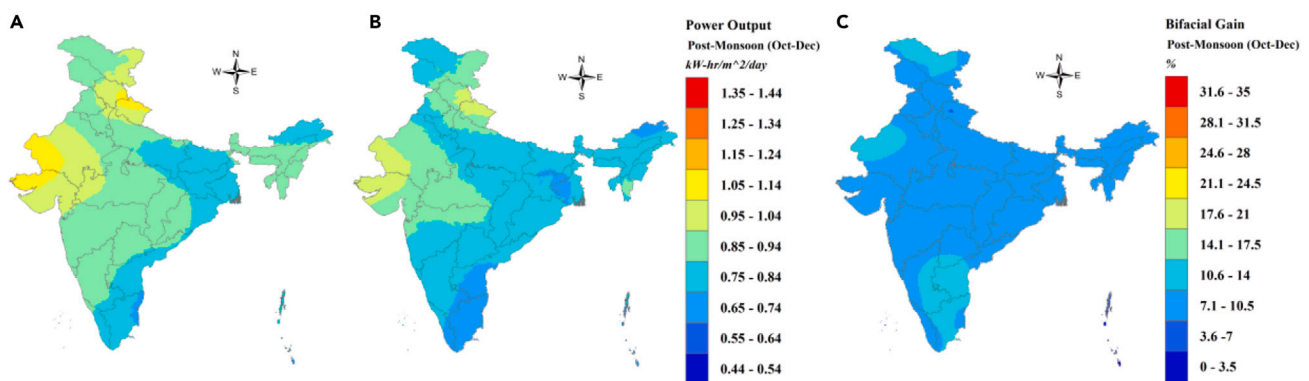


Figure 8. Power output and bifacial gain maps for the post-monsoon season in India (Oct-Dec)

- (A) Bifacial power output.
- (B) Monofacial power output.
- (C) Bifacial gain.

Table 2. Indian zone wise variation in bifacial gain

Range of bifacial gain (%)					
Indian Zones	Winter season (Jan–Feb)	Pre-monsoon season (Mar–May)	South-west monsoon season (Jun–Sep)	Post-monsoon season (Oct–Dec)	Annual (Jan–Dec)
North Zone	7.8–26.5	9.4–32.5	10.3–19.7	5.8–15.9	9.4–22.3
Middle Zone	4.9–13.7	6.6–18.6	9.1–19.7	6.0–10.3	7.9–14.2
East Zone	7.2–20.7	9.4–27.8	13.1–21.9	7.2–13.1	9.9–20.7
West Zone	6.6–12.9	6.0–14.3	7.8–16.6	6.8–12.0	7.4–14.2
South Zone	2.1–11.8	1.9–11.4	2.0–15.8	2.6–12.9	2.4–13.0

It can be observed from Figure 9 that higher ground albedo gives better bifacial gain in south zone and the lower values for parts of west and north zone of India. This may be due to the higher amount of diffuse radiation in the south zone compared to parts of west and north zones. It can be inferred that the potential of bifacial PV can be improved by artificially enhancing the ground albedo like painting the roof top with white weather coating, covering ground with reflective materials, etc. The bifacial PV potential can be improved significantly anywhere in India by enhancing the ground albedo at that location.

Effect of height

The effect of installation height from ground/roof is studied by keeping all other parameters fixed at optimal value with a ground albedo of 15% and varying the height. Since the position of Sun in the horizon influences the bifacial gain, the study was carried out for summer solstice (June 21), winter solstice (December 22), equinox 1 (March 21), and equinox 2 (September 22). The hourly radiation data of these days at Delhi location are input in the model and the bifacial gain at noon for varying heights is plotted in Figure 10.

The bifacial gain is found to first increase and then stabilize with the increase in height. The initial increase in bifacial gain is due to the larger view factor values from the increase in the area of ground influencing the reflected radiation with height. The best bifacial gain was obtained between a height of 1 and 2.5 m with respect to the position of the Sun in the horizon. Effective increase in bifacial gains was observed when the height was raised up to 1–1.5 m on all days. A similar pattern was observed at other locations in India. An optimal height of 1.5 m is suggested in India for the best year-round performance of bifacial PV.

DISCUSSION

India needs to accelerate the market entry of bifacial PV technology to meet its 7th UN SDG goal. Since the performance of bifacial PV depends on parameters like latitude, slope, pitch, height, and albedo at any location in addition to solar radiation, a solar radiation data map of India alone will not be able to predict the best locations for bifacial PV installations. So, it is the need of the hour to develop an optimized resource potential map for bifacial PV to spearhead the growth of bifacial PV in Indian market.

However, there are only a very few small-scale bifacial installations of bifacial PV and scarce performance data for the Indian scenario compared to monofacial PV. To overcome this, a bifacial PV model was developed and validated with experimental data. The optimal parameters for installation at any location were also predicted from the model. Bifacial PV performance for 188 locations in India was simulated and maps were developed by Kriging interpolation on ArcMap. The major findings of the study are as follows.

- Daily average bifacial power output is much higher for bifacial PV (0.6–1.2 kWh/m²/day) compared to monofacial PV (0.5–1 kWh/m²/day). Daily average annual bifacial power output potential was the highest in west and parts of north zone and least in the east zone.

Table 3. Albedo range for different types of surfaces

Sl. No	Type of surface	Albedo (%)
1	Snow	42–96
2	White Sand	58–62
3	Ice	31–39
4	Sand	21–43
5	Concrete	20–40
6	Soil	21–35
7	Grass	10–25
8	Asphalt	9–18
9	Water	6–9

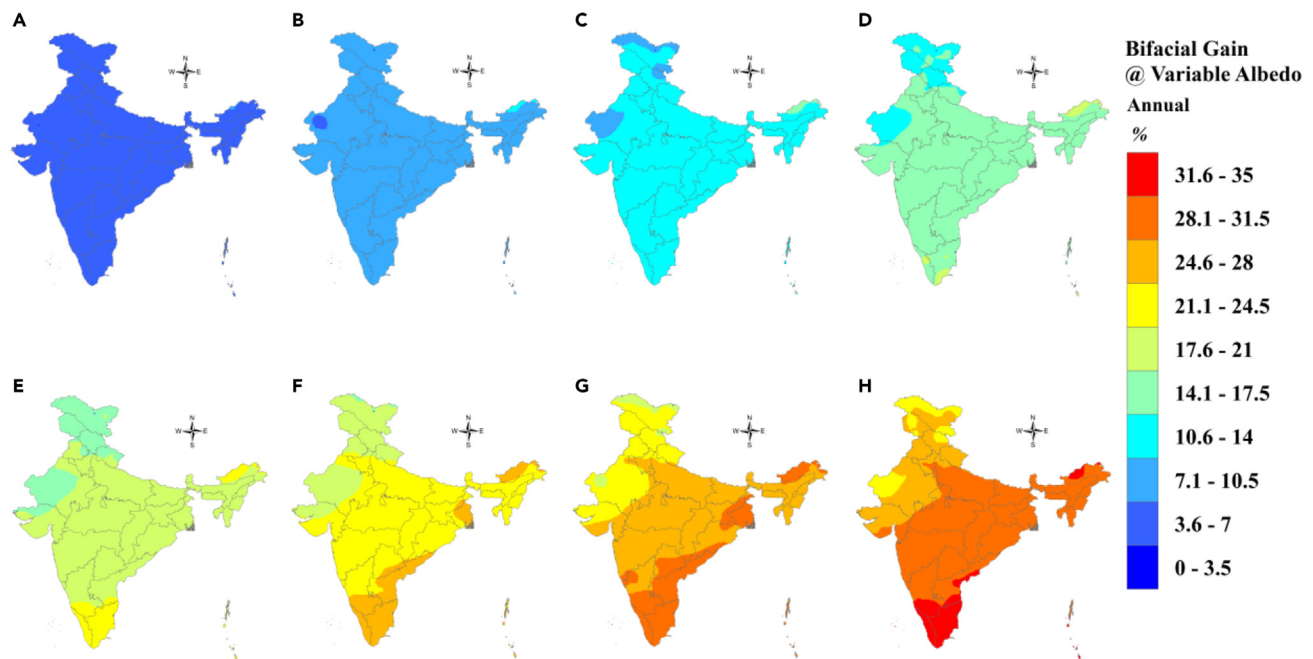


Figure 9. Bifacial gain maps for varying ground albedo

- (A) Ground albedo of 5%.
 (B) Ground albedo of 10%.
 (C) Ground albedo of 15%.
 (D) Ground albedo of 20%.
 (E) Ground albedo of 35%.
 (F) Ground albedo of 30%.
 (G) Ground albedo of 35%.
 (H) Ground albedo of 40%.

- The annual average bifacial gain at optimal parameters of installation was between 2.4% and 22.3%. The highest annual average bifacial gain is in the north zone of India, while the lowest gain is in the Andaman and Nicobar Islands in the south zone of India.
- The seasonal performance of bifacial PV was also studied. The highest bifacial power output of 1.42 kWh/m²/day and bifacial gain of 32.5% was obtained during the pre-monsoon season, while the least bifacial power generation of 0.52 kWh/m²/day occurs in the south-west monsoon season.
- The bifacial gain was found to linearly increase with an increase in ground albedo. Therefore, it is suggested to install bifacial panels on surfaces with higher values of albedo for best performance.
- An optimal height of 1.5 m is suggested in India for the best year-round performance of bifacial PV.

Limitations of the study

The model was validated experimentally for the Chennai location only due to the unavailability of bifacial PV data from other locations. However, using PVsyst, the model was validated for five locations. The average percentage deviation of hourly power generated by the 100 kWp power plant between PVsyst and the proposed model at various locations throughout India was found to vary between 2% and 7%.

Soiling losses are another important parameter that affects the performance of PV panels, which vary geographically and seasonally. The soiling losses are neglected in the development of maps.

Also, electrical transmission DC and AC wire losses and mismatch losses were also neglected as these factors vary depending on the design and capacity of the power plants.

STAR★METHODS

Detailed methods are provided in the online version of this paper and include the following:

- [KEY RESOURCES TABLE](#)
- [RESOURCE AVAILABILITY](#)
 - Lead contact

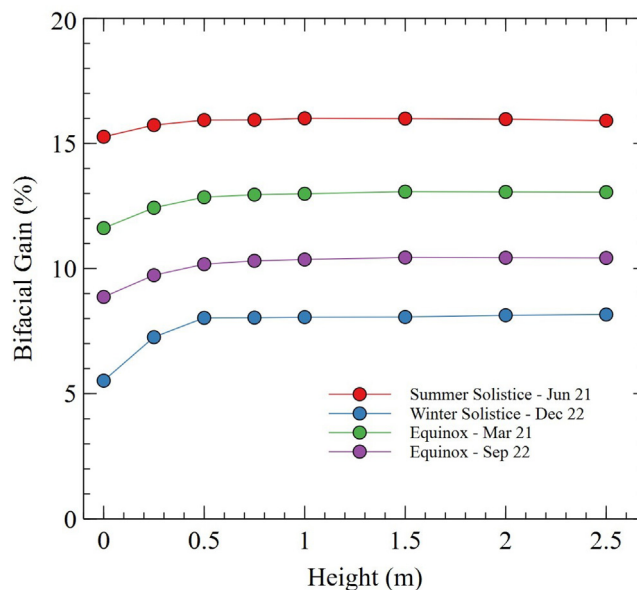


Figure 10. Effect of height on bifacial PV performance

- Materials availability
- Data and code availability
- EXPERIMENTAL MODEL AND SUBJECT DETAILS
- METHOD DETAILS
 - Methodology
 - Modeling of bifacial PV
 - Electro-thermal model
 - Photovoltaic Array Performance Model
 - Single-diode model
 - Experimental Validation of the model
 - Validation of model with PVsyst
 - Map development in ArcMap software
- QUANTIFICATION AND STATISTICAL ANALYSIS
- ADDITIONAL RESOURCES

SUPPLEMENTAL INFORMATION

Supplemental information can be found online at <https://doi.org/10.1016/j.isci.2023.108017>.

ACKNOWLEDGMENTS

The authors would like to thank the financial support for the project titled “A novel Bifacial Photovoltaic Thermal (BPVT) System for enhanced solar drying application” funded under the Selective Excellence Initiative, Directorate of Research, SRM Institute of Science and Technology, Kattankulathur Campus, Chennai, Tamil Nadu, India.

The authors would like to acknowledge Daystar Solar, Anna Nagar East, Chennai, Tamil Nadu, for their support in the development and installation of the bifacial PV test bed.

AUTHOR CONTRIBUTIONS

J.J.: conceptualization, methodology, development of model and bifacial PV system, model simulation, system and model testing, data generation, map development, writing – original draft preparation. S.M.: conceptualization, development of model, writing – review & editing, supervision, funding acquisition.

DECLARATION OF INTERESTS

The authors declare that they have no known competing financial interests or personal relationships that could have appeared to influence the work reported in this paper.

Received: May 12, 2023
Revised: August 29, 2023
Accepted: September 18, 2023
Published: September 22, 2023

REFERENCES

- <https://sdgs.un.org/goals/goal7>.
- <https://www.niti.gov.in/reports-sdg>.
- <https://unfccc.int/sites/default/files/NDC/2022-08/India%20Updated%20First%20Nationally%20Determined%20Contrib.pdf>.
- <https://mnre.gov.in/solar/current-status/>.
- Singh, S.K., and Chander, N. (2022). Mid-life degradation evaluation of polycrystalline Si solar photovoltaic modules in a 100 kWp grid-tied system in east-central India. *Renew. Energy* 199, 351–367. <https://doi.org/10.1016/j.renene.2022.09.013>.
- http://ncpre.iitb.ac.in/ncpre/research/pdf/All_India_Survey_of_Photovoltaic_Module_Reliability_2018_Report.pdf.
- Diniz AS, Costa SC, Kazmerski LL. Photovoltaic Technology: Advances in Solar Cells and Modules
- Jean, J., Woodhouse, M., and Bulović, V. (2019). Accelerating Photovoltaic Market Entry with Module Replacement. *Joule* 3, 2824–2841. <https://doi.org/10.1016/j.joule.2019.08.012>.
- Gu, W., Ma, T., Ahmed, S., Zhang, Y., and Peng, J. (2020). A comprehensive review and outlook of bifacial photovoltaic (bPV) technology. *Energy Convers. Manag.* 223, 113283. <https://doi.org/10.1016/j.enconman.2020.113283>.
- Kopecek, R., and Libal, J. (2021). Bifacial Photovoltaics 2021: Status, Opportunities and Challenges. *Energies (Basel)* 14, 2076. <https://doi.org/10.3390/en14082076>.
- Pal, S., Reinders, A., and Saive, R. (2020). Simulation of Bifacial and Monofacial Silicon Solar Cell Short-Circuit Current Density Under Measured Spectro-Angular Solar Irradiance. *IEEE J. Photovoltaics* 10, 1803–1815. <https://doi.org/10.1109/jphotov.2020.3026141>.
- Gu, W., Li, S., Liu, X., Chen, Z., Zhang, X., and Ma, T. (2021). Experimental investigation of the bifacial photovoltaic module under real conditions. *Renew. Energy* 173, 1111–1122. <https://doi.org/10.1016/j.renene.2020.12.024>.
- <https://www.vdma.org/international-technology-roadmap-photovoltaic>.
- Eguren, J., Martínez-Moreno, F., Merodio, P., and Lorenzo, E. (2022). First bifacial PV modules early 1983. *Sol. Energy* 243, 327–335. <https://doi.org/10.1016/j.solener.2022.08.002>.
- Tang, H.B., Ma, S., Lv, Y., Li, Z.P., and Shen, W.Z. (2020). Optimization of rear surface roughness and metal grid design in industrial bifacial PERC solar cells. *Sol. Energy Mater. Sol. Cell.* 216, 110712. <https://doi.org/10.1016/j.solmat.2020.110712>.
- Chawarambwa, F.L., Putri, T.E., Attri, P., Kamataki, K., Itagaki, N., Koga, K., and Shiratani, M. (2021). Highly efficient and transparent counter electrode for application in bifacial solar cells. *Chem. Phys. Lett.* 768, 138369. <https://doi.org/10.1021/acsami.7b17815.s001>.
- Onno, A., Rodkey, N., Asgharzadeh, A., Manzoor, S., Yu, Z.J., Toor, F., and Holman, Z.C. (2020). Predicted Power Output of Silicon-Based Bifacial Tandem Photovoltaic Systems. *Joule* 4, 580–596. <https://doi.org/10.1016/j.joule.2019.12.017>.
- Ingenito, A., Allebé, C., Libraro, S., Ballif, C., Paviet-Salomon, B., Nicolay, S., and Diaz Leon, J.J. (2023). 22.8% full-area bifacial n-PERT solar cells with rear side sputtered poly-Si(n) passivating contact. *Sol. Energy Mater. Sol. Cell.* 249, 112043. <https://doi.org/10.1016/j.solmat.2022.112043>.
- Raina, G., and Sinha, S. (2022). A holistic review approach of design considerations, modelling, challenges and future applications for bifacial photovoltaics. *Energy Convers. Manag.* 271, 116290. <https://doi.org/10.1016/j.enconman.2022.116290>.
- Campana, P.E., Stridh, B., Amaducci, S., and Colauzzi, M. (2021). Optimisation of vertically mounted agrivoltaic systems. *J. Clean. Prod.* 325, 129091. <https://doi.org/10.1016/j.jclepro.2021.129091>.
- <https://www.nrel.gov/docs/fy22osti/82540.pdf>.
- Rodríguez-Gallegos, C.D., Bieri, M., Gandhi, O., Singh, J.P., Reindl, T., and Panda, S.K. (2018). Monofacial vs bifacial Si-based PV modules: Which one is more cost-effective? *Sol. Energy* 176, 412–438. <https://doi.org/10.1016/j.solener.2018.10.012>.
- Rodríguez-Gallegos, C.D., Liu, H., Gandhi, O., Singh, J.P., Krishnamurthy, V., Kumar, A., Stein, J.S., Wang, S., Li, L., Reindl, T., and Peters, I.M. (2020). Global Techno-Economic Performance of Bifacial and Tracking Photovoltaic Systems. *Joule* 4, 1514–1541. <https://doi.org/10.1016/j.joule.2020.05.005>.
- <https://www.pv-magazine.com/2020/08/19/bifacial-modules-the-challenges-and-advantages/>.
- <https://pvwatts.nrel.gov/>.
- <https://pvsol-online.valentin-software.com/#/>.
- Patel, M.T., Khan, M.R., Sun, X., and Alam, M.A. (2019). A worldwide cost-based design and optimization of tilted bifacial solar farms. *Appl. Energy* 247, 467–479. <https://doi.org/10.1016/j.apenergy.2019.03.150>.
- Guerrero-Lemus, R., Vega, R., Kim, T., Kimm, A., and Shephard, L.E. (2016). Bifacial solar photovoltaics – A technology review. *Renew. Sustain. Energy Rev.* 60, 1533–1549. <https://doi.org/10.1016/j.rser.2016.03.041>.
- Gu, W., Ma, T., Li, M., Shen, L., and Zhang, Y. (2020). A coupled optical-electrical-thermal model of the bifacial photovoltaic module. *Appl. Energy* 258, 114075. <https://doi.org/10.1016/j.apenergy.2019.114075>.
- Mahtta, R., Joshi, P.K., and Jindal, A.K. (2014). Solar power potential mapping in India using remote sensing inputs and environmental parameters. *Renew. Energy* 71, 255–262. <https://doi.org/10.1016/j.renene.2014.05.037>.
- <http://164.100.94.214/india-solar-resource-maps>.
- <https://www.arcgis.com/index.html>.
- <https://power.larc.nasa.gov/data-access-viewer/>.
- Ichoku, C. (2018). NASA Visible Earth Catalog. <https://visibleearth.nasa.gov/view.php?id=60636>.
- Pelaez, S.A., Deline, C., Greenberg, P., Stein, J.S., and Kostuk, R.K. (2019). Model and Validation of Single-Axis Tracking With Bifacial PV. *IEEE J. Photovoltaics* 9, 715–721. <https://doi.org/10.1109/jphotov.2019.2892872>.
- https://mausam.imd.gov.in/imd_latest/contents/ar2022.pdf.
- https://www.lg.com/global/business/download/resources/solar/Bifacial_design_guide_Full_ver.pdf.
- Appelbaum, J. (2018). The role of view factors in solar photovoltaic fields. *Renew. Sustain. Energy Rev.* 81, 161–171. <https://doi.org/10.1016/j.rser.2017.07.026>.
- Kratovichil, J., Boyson, W., and King, D. (2004). Photovoltaic array performance model. <https://doi.org/10.2172/919131>.
- Tian, H., Mancilla-David, F., Ellis, K., Muljadi, E., and Jenkins, P. (2012). A cell-to-module-to-array detailed model for photovoltaic panels. *Sol. Energy* 86, 2695–2706. <https://doi.org/10.1016/j.solener.2012.06.004>.
- Oliver, M.A., and Webster, R. (1990). Kriging: a method of interpolation for geographical information systems. *Int. J. Geogr. Inf. Syst.* 4, 313–332. <https://doi.org/10.1080/02693799008941549>.
- Aoun, N. (2022). Methodology for predicting the PV module temperature based on actual and estimated weather data. *Energy Convers. Manag.* 14, 100182. <https://doi.org/10.1016/j.ecmx.2022.100182>.
- Hansen, C., Riley, D., Deline, C., Toor, F., and Stein, J. (2017). A Detailed Performance Model for Bifacial PV Modules (Sandia National Lab.(SNL-NM)).
- Urrejola, E., Valencia, F., Fuentealba, E., Deline, C., Pelaez, S., Meybray, J., et al. (2020). bifPV2020 Bifacial Workshop: A Technology Overview. <https://doi.org/10.2172/1710156>.
- <https://www.pv-magazine.com/2020/02/19/discussing-bifacial-project-economics/>.
- Trial Version. <https://www.pvsyst.com/download-pvsyst/>.
- Kleijnen, J.P. (2009). Kriging metamodelling in simulation: A review. *Eur. J. Oper. Res.* 192, 707–716. <https://doi.org/10.1016/j.ejor.2007.10.013>.

STAR★METHODS

KEY RESOURCES TABLE

REAGENT or RESOURCE	SOURCE	IDENTIFIER
Software and algorithms		
MATLAB	MathWorks	https://www.mathworks.com/products/matlab.html
Spyder (Python)	Anaconda	https://www.anaconda.com/download
PVsys	PVsys	https://www.pvsyst.com/
ArcMap or ArcGIS	esri	https://pro.arcgis.com/en/pro-app/latest/get-started/download-arcgis-pro.htm

RESOURCE AVAILABILITY

Lead contact

Further information and requests for resources should be directed to and will be fulfilled by the lead contact, Dr. S. Manikandan (manikans@smist.edu.in).

Materials availability

All solar panels, materials and balance of the system can be procured commercially.

This study did not generate new unique reagents.

Data and code availability

- All software used in this study is described in the [method details](#) and [key resources table](#).
- All original codes used in the model have been reported in the [supplemental information](#) (Methods S1 and S2).
- Any additional information required to reanalyze the data reported in this work paper is available from the [lead contact](#) upon request.

EXPERIMENTAL MODEL AND SUBJECT DETAILS

No experimental model was used in this work. The specific experimental details are provided in the [method details](#).

METHOD DETAILS

Methodology

[Figure S1](#) gives the flow diagram for the bifacial PV map generation process. A view factor model for the bifacial PV field was developed and used to generate maps to predict the bifacial PV potential of India. The model was experimentally validated using a bifacial PV test bed. The model was developed using all relevant view factors found by applying the cross-string rule by Hottel.³⁸ For bifacial PV, the amount of the diffused and reflected radiation on the front and rear sides of the collector depends on the view factor of the collector to the sky, to the ground, and to the surrounding objects. The model used solar geometry and the MATLAB program to evaluate the total radiation incident on the front and rear sides of the bifacial PV panels. The model was experimentally validated by a bifacial PV test bed at SRM Institute of Science and Technology, Chennai, India.

To develop the maps, the optimal orientation of bifacial PV ([Table 1](#)) and solar radiation, surface albedo, wind speed and ambient temperature are taken from NASA's Power Data Access Viewer³³ for 188 locations in India and are given as input to the view factor model. The front and rear side irradiation on the panel is evaluated from the view factor model, and the cell temperature is obtained by the Photovoltaic Array Performance Model.³⁹ These data and monofacial and bifacial PV panel characteristics are imported to the Single-diode model to account for electrical and thermal corrections.^{29,40} The yearly and seasonal data predicted at 188 coordinate locations are input to the shape file of India in ArcMap software. Spatial analysis was done by Kriging interpolation to generate the bifacial PV maps.⁴¹ In addition, the performance of bifacial PV with the variation in height and ground albedo was also studied.

Modeling of bifacial PV

A view factor model was developed using the Cross String rule by Hottel. The PV panel field is idealized as an infinite number of rows of panels. Each row in the field consists of continuous infinite length, neglecting the spacing between the panels, including the edges of support frames. The ground is assumed to be a Lambertian surface of shaded and unshaded regions formed by panels self-shading on the ground. The model

accurately predicts the hourly and seasonal variation of the panels' shadow based on the Sun position on the horizon from the solar angles. The model also determines the effect of orientation parameters like slope (β), height (H), pitch (P), and ground albedo on the performance of bifacial panels. The unshaded regions within a pitch are represented by USP1 and USP2 and the shaded region is represented by SP as in Figure S2. The abbreviations of all symbols used are given in Table S1.

The total radiation falling on a PV panel is the sum of the beam, diffuse, and reflected radiation. The total irradiation falling on the front side of a PV module is given by Equation 1 and represents the total irradiation falling on a monofacial PV panel.

$$G_{Pn}^f = (GHI - DHI) \times R_b^f + DHI \times F_{Pn \rightarrow sky}^f + \sum_1^X [GHI \times \rho_g \times F_{Pn \rightarrow USPn}^f + DHI \times \rho_g \times F_{Pn \rightarrow SPn}^f] + G_{Pn-1}^f \times \rho_p \times F_{Pn \rightarrow Pn-1}^f \quad (\text{Equation 1})$$

where, GHI is the global horizontal irradiance, DHI is the diffuse horizontal irradiance, R_b^f is the ratio of front tilted irradiance to horizontal irradiance, ρ_g is the reflectivity of the ground, $F_{Pn \rightarrow sky}^f$ is the view factor of the front side of the panel, and sky dome, $F_{Pn \rightarrow USPn}^f$ is the view factor of the unshaded region and the front side of the panel, G_{Pn-1}^f is the irradiation falling on the rear side of the panel in the front, ρ_p is the reflectivity of the panels, $F_{Pn \rightarrow Pn-1}^f$ view factor between the front of nth panel row and rear side of (n-1)th panel row, X is the number of rows of panels influencing the reflected irradiation falling on the front side of the panel and n is the number of row of bifacial PV collector.

R_b^f is as follows

$$R_b^f = \begin{cases} \frac{\cos \theta^f}{\cos \theta_z^f}, & \gamma - \pi/2 \leq \omega \leq \gamma + \pi/2 \\ 0, & \omega < \gamma - \pi/2 \text{ or } \omega > \gamma + \pi/2 \end{cases} \quad (\text{Equation 2})$$

where, θ^f is the angle of incidence, θ_z^f is the zenith angle, γ is the surface azimuth angle, and ω is the hour angle.

Similarly, the total irradiation falling on the rear side of the PV module is given by:

$$G_{Pn}^r = (GHI - DHI) \times R_b^r + DHI \times F_{Pn \rightarrow sky}^r + \sum_1^Y [GHI \times \rho_g \times F_{Pn \rightarrow USPn}^r + DHI \times \rho_g \times F_{Pn \rightarrow SPn}^r] + G_{Pn+1}^f \times \rho_p \times F_{Pn \rightarrow Pn+1}^r \quad (\text{Equation 3})$$

where, R_b^r is the ratio of rear tilted irradiance to horizontal irradiance, $F_{Pn \rightarrow sky}^r$ is the view factor of the rear side of the panel, and sky dome, $F_{Pn \rightarrow USPn}^r$ is the view factor of the unshaded region and rear side of the panel, $F_{Pn \rightarrow SPn}^r$ is the view factor of the shaded region and rear side of the panel, and $F_{Pn \rightarrow Pn+1}^r$ is the view factor between the rear side of nth panel row and the front side of (n+1)th panel row.

R_b^r is represented by Equation 4 as

$$R_b^r = \begin{cases} 0, & \gamma - \pi/2 \leq \omega \leq \gamma + \pi/2 \\ \frac{\cos \theta^r}{\cos \theta_z^r}, & \omega < \gamma - \pi/2 \text{ or } \omega > \gamma + \pi/2 \end{cases} \quad (\text{Equation 4})$$

where, θ^r is the angle of incidence and θ_z^r is the zenith angle on the rear side of the panel.

The view factors in Equations 1 and 3 are evaluated for the field of bifacial PV panels for all shaded and unshaded regions. A Matlab™ program (Method S1) is developed to evaluate the individual view factors of the reference row of panels with each adjacent row of panels in an incremental mode, and then the cumulative view factors are evaluated.

From the view factor model, the total radiation falling on the front and rear side of the PV panel is evaluated.

Electro-thermal model

The performance of the bifacial PV module decreases with an increase in temperature above Standard Test Condition (STC). The temperature for testing PV modules at STC is only 25°C. India is predominantly tropical and has the typical feature of high temperatures above STC conditions almost throughout the year. The real-time efficiency of the solar PV panels will be lower than at STC conditions. The temperature of a panel at any location depends on various parameters like ambient temperature, radiation incident, wind velocity, etc.⁴²

Photovoltaic Array Performance Model

The photovoltaic cell temperature of bifacial module was determined by the Photovoltaic Array Performance Model³⁹ using an approach similar to monofacial modules. The accuracy of this model for bifacial PV was experimentally determined by measuring the temperature with thermocouples attached in between cells on a bifacial module's rear-surface in parallel with ambient temperature and wind speed.⁴³

The cell temperature inside the module is evaluated as a function of back-surface temperature and a predetermined temperature difference between the back surface and the cell that depends on the type of Module. The empirical equation to determine cell temperature is

$$T_c = T_m + \frac{(G_{pn}^f + G_{pn}^r)}{G_{pn}^{ref}} \times \Delta T \quad (\text{Equation 5})$$

where, T_c is the cell temperature in module ($^{\circ}\text{C}$), T_m is the module surface temperature ($^{\circ}\text{C}$), G_{pn}^f is the solar irradiance on the front side of module in W/m^2 Equation 1, G_{pn}^r is the solar irradiance on the rear side of module in W/m^2 Equation 3, G_{pn}^{ref} is the reference solar irradiance on the module at $1000 \text{ W}/\text{m}^2$, and ΔT is the standard temperature difference between the cell and module back surface at an irradiance level of $1000 \text{ W}/\text{m}^2$. For a glass-cell-glass bifacial module in an open rack mount arrangement ΔT is 3°C .⁴³

An empirical relation Equation 6 gives the module surface temperature, which is a function of ambient temperature, total irradiation, and wind speed.

$$T_m = (G_{pn}^f + G_{pn}^r) \times [e^{a+b \cdot WS}] + T_a \quad (\text{Equation 6})$$

where, T_m is the module surface temperature in $^{\circ}\text{C}$, T_a is the ambient air temperature at the location in $^{\circ}\text{C}$, WS is the standard wind speed measured at 10 m height in m/s, a is the empirically-determined coefficient establishing the upper limit for module temperature at low wind speeds and high solar irradiance and b is empirically-determined coefficient establishing the rate at which module temperature drops as wind speed increases. For a glass-cell-glass bifacial module in an open rack mount arrangement $a = -3.47$ and $b = -0.0594$.⁴³

The above electro-thermal model can be modified for a Glass-cell-polymer sheet monofacial module in an open rack mount arrangement with input parameters $G_{pn}^r = 0$, $\Delta T = 3^{\circ}\text{C}$, $a = -3.56$, and $b = -0.0750$ in the Equations 8 and 9.³⁹

Single-diode model

The single-diode model of a PV cell is used to evaluate the power output of monofacial and bifacial PV.^{29,40} Figure S3 represents the equivalent circuit of a solar cell. From the equivalent circuit, the Shockley diode mathematical model of a PV cell was derived as in Equation 7.

$$I = I_{ph} - I_d - I_p = I_{ph} - I_0 \left[\exp\left(\frac{V+I \times R_s}{V_t}\right) - 1 \right] - \frac{V+I \times R_s}{R_p} \quad (\text{Equation 7})$$

where, I_{ph} is the photo current, I_d is the diode current, I_p is the current through the parallel resistance, I_0 is the diode reserve saturation current, R_s is the series resistance, R_p is the parallel resistance and V_t is the diode thermal voltage.

The Shockley diode equation based mathematical model of a PV cell can be modified for Standard Test Conditions (STC) as Equation 8

$$I = I_{ph,ref} - I_{0,ref} \left[\exp\left(\frac{V+I \times R_{s,ref}}{N_s \times V_{t,ref}}\right) - 1 \right] - \frac{V+I \times R_{s,ref}}{R_{p,ref}} \quad (\text{Equation 8})$$

where, $I_{ph,ref}$, $I_{0,ref}$, $R_{s,ref}$, $R_{p,ref}$, and $V_{t,ref}$ are the parameters at STC and N_s is the number of solar cells connected in series.

The diode thermal voltage is evaluated by

$$V_{t,ref} = i \times K \times T_{ref} / q \quad (\text{Equation 9})$$

i is the diode ideality factor, q is electronic charge ($1.602\text{E}-19 \text{ C}$), K is the Boltzmann's constant ($1.381\text{E}-23 \text{ J/K}$), and T_{ref} is the temperature at STC (25°C).

The five parameters $V_{t,ref}$, $I_{ph,ref}$, $I_{0,ref}$, $R_{s,ref}$ and $R_{p,ref}$ are unknown parameters which are not available from the data sheet provided by the manufacturer. These parameters are obtained under STC and then further evaluated for non-STC from the radiation data and cell temperature obtained from the Photovoltaic Array Performance Model.

Parameters at STC

Thermal voltage at STC is given by Equation 10

$$V_{t,ref} = \frac{\beta \times T_{ref} - V_{oc,ref}}{\frac{N_s \times T_{ref} \times \alpha}{I_{ph,ref}} - 3 \times N_s - \frac{E_g \times N_s}{K \times T_{ref}}} \quad (\text{Equation 10})$$

where, α is the temperature coefficient of short circuit current, β is the voltage temperature coefficient and E_g is the bandgap ($1.7936\text{e}-19 \text{ J}$).

The photo current at STC is obtained by taking $V = 0$ in Equation 8,

$$I_{ph,ref} \approx I_{sc,ref} \quad (\text{Equation 11})$$

The diode reserve saturation current at STC is obtained by taking $I = 0$ in Equation 8,

$$I_{0,ref} = I_{sc,ref} \times \exp\left(\frac{-V_{oc,ref}}{N_s \times V_{t,ref}}\right) \quad (\text{Equation 12})$$

The parallel resistance at STC is given by Equation 13,

$$R_{p,ref} = \frac{(V_{mp,ref} - I_{mp,ref} \times R_{s,ref}) \times (V_{mp,ref} - N_s \times V_{t,ref})}{(V_{mp,ref} - I_{mp,ref} \times R_{s,ref}) \times (I_{sc,ref} - I_{mp,ref}) - (N_s \times V_{t,ref} \times I_{mp,ref})} \quad \text{(Equation 13)}$$

where $V_{mp,ref}$ and $I_{mp,ref}$ are the voltage and current at the Maximum Power Point (MPP) at STC.

The series resistance at STC is given by Equation 14,

$$I_{mp,ref} = I_{ph,ref} - I_{0,ref} \left[\exp\left(\frac{V_{mp,ref} + I_{mp,ref} \times R_{s,ref}}{N_s \times V_{t,ref}}\right) - 1 \right] - \left[\frac{(V_{mp,ref} + I_{mp,ref} \times R_{s,ref}) [(V_{mp,ref} - I_{mp,ref} \times R_{s,ref}) \times (I_{sc,ref} - I_{mp,ref}) - (N_s \times V_{t,ref} \times I_{mp,ref})]}{(V_{mp,ref} - I_{mp,ref} \times R_{s,ref}) \times (V_{mp,ref} - N_s \times V_{t,ref})} \right] \quad \text{(Equation 14)}$$

Parameters at non-STC

The equivalent parameters at non-STC conditions V_t , I_{ph} , I_0 , R_s and R_p are calculated from Equations 15, 16, 17, 18, 19, 20, and 21.

$$I_{ph} = \frac{G_E^p}{G_{pn}^{ref}} (I_{ph,ref} + \alpha \times (T - T_{ref})) \quad \text{(Equation 15)}$$

$$I_0 = I_{0,ref} \left(\frac{T}{T_{ref}}\right)^3 \exp\left[\frac{q \times E_g}{K} \left(\frac{1}{T_{ref}} - \frac{1}{T}\right)\right] \quad \text{(Equation 16)}$$

$$R_s = R_{s,ref} \quad \text{(Equation 17)}$$

$$R_p = \frac{G_{pn}^{ref}}{G_E^p} R_{p,ref} \quad \text{(Equation 18)}$$

$$V_t = \frac{T}{T_{ref}} V_{t,ref} \quad \text{(Equation 19)}$$

where, G_E^p is the total irradiance falling on the panel given by

$$G_E^p = G_{pn}^f + G_{pn}^r \times \varphi \quad \text{(Equation 20)}$$

where, φ is the bifaciality factor of a PV cell or module which is the ratio of maximum power or short circuit current produced by the front side to the rear side of the panel at STC, given by

$$\varphi = \begin{cases} \min\left(\frac{I_{sc,ref,R}}{I_{sc,ref,F}}, \frac{P_{max,ref,R}}{P_{max,ref,F}}\right); & \text{Bifacial Module} \\ 0; & \text{Monofacial Module} \end{cases} \quad \text{(Equation 21)}$$

The bifaciality factor of PV modules varies between 60% to 90% and above, based on the technology used. P-type bifacial PERC has a bifaciality factor of 60%, and n-type passivated emitter rear totally diffused (PERT) and heterojunction (HJT) panels have a value of 90% and above. The utility scale bifacial modules have a bifaciality factor in the range of 60% - 70%.^{44,45} In this research, the bifaciality factor of 70% is considered for the development of maps.

The current and voltage at non-STC is obtained by replacing the equivalent parameters in Equation 7. A Python code (Method S2) is developed to solve the above formulae to find the actual panel power output. The monofacial and bifacial PV specifications from the manufacturer data sheets of the PV panels. The Equations 7, 8, 9, 10, 11, 12, 13, and 14 is solved by fsolve inputting initial guess values to solve for the maximum current and voltage at STC and then generate values at non-STC by Equations 15, 16, 17, 18, 19, 20, and 21. The predicted IV-characteristics of the monofacial and bifacial at STC by the single-diode model were the same as the manufacturer data sheet at STC.

The monofacial and bifacial PV panel power output at maximum power point is evaluated as

$$P_{PV} = I_{mp} \times V_{mp} \quad \text{(Equation 22)}$$

The monofacial and bifacial power output is separately evaluated as P_{mPV} and P_{bPV} respectively from the single diode model.

The bifacial gain is the percentage improvement in power output of a bifacial PV panel with respect to a monofacial panel, and the B.G is given by Equation 23

$$B.G = \left[\frac{P_{bPV} - P_{mPV}}{P_{mPV}} \right] \times 100 \quad (\text{Equation 23})$$

Experimental Validation of the model

A bifacial PV test bed was developed at SRM Institute of Science and Technology Campus, Chennai, Tamil Nadu, India (12.8205007° N, 80.039724° E) as in [Figure S4](#) to validate the model. The test bed consisted of three bifacial PV panels (Monocrystalline Nexus Bifacial 200 Watt) (Panel 1 - 3) and a monofacial PV panel (Mono PERC SunSolar 200 Watt) (Panel 4) of 200 Wp. The specifications of the panels are given in [Table S2](#). The test bed was designed to vary and test individual factors like slope, pitch, and height of bifacial PV. GP2 Advanced Data Logger and controller weather station measured the radiation data and climate. Luminous NXG 1150 Pure Sine Wave Solar Inverter with a 160Ah Tubular Lead Acid Battery and an incandescent lighting load of 300 W constituted the balance of the system. The current and voltage output of the four panels was measured by an Arduino-based data logger.

The ground albedo, i.e., the reflectivity of roof tiles, was determined using UV-Vis Spectrometer (UV 3600 PLUS, SHIMADZU). The average reflectivity of roof tiles is 17.013% over the wavelength range of 200 nm to 1200 nm, as shown in [Figure S5](#).

During the test, panels were oriented at optimal model specification as in [Table 1](#). The panels were arranged with a slope of 13°, GCR of 0.4, pitch of 2 m and ground albedo of 17.013%. The power output and the bifacial gain were obtained from the data logger. The power output and bifacial gain were also simulated from the model at similar conditions. [Figure S6A](#) gives the power output from the actual monofacial and bifacial PV panels with the corresponding models, and [Figure S6B](#) gives the bifacial gain of the panels and the model. The power output predicted by the model is slightly higher than the actual system. The model predicted the power output with a root mean square error of 3.88 W and bifacial gain with a root mean square error of 2.74%.

Validation of model with PVsyst

The proposed model was further validated with commercially available PVsyst software.⁴⁶ The PVsyst and proposed model were given the same input of a 100 kWp bifacial PV power plant located in five locations. Bifacial PV simulation was done using an unlimited sheds 2D-model in PVsyst for the PV panels of specifications as in [Table S3](#). The hourly power output by the proposed model and PVsyst at five different locations are presented in [Figures S7–S11](#). The average percentage deviation of hourly power generated by the 100 kWp power plant between PVsyst and the proposed model at various locations throughout India was found to vary between 2% to 7%.

Map development in ArcMap software

Bifacial PV maps of India was developed using ArcMap software. ArcMap is a smart, interactive, and data-driven mapping software. Bifacial PV simulation data obtained from the model at 188 locations in India was input into ArcMap. Spatial analysis was done by Kriging interpolation,⁴⁷ and bifacial PV resource maps were developed.

QUANTIFICATION AND STATISTICAL ANALYSIS

To develop the bifacial PV maps, the monthly average and yearly average data was used from NASA's Power Data Access Viewer. Spatial analysis of data from 188 locations was done by Kriging interpolation to develop the maps.

ADDITIONAL RESOURCES

No additional resources were generated from the study.